Journal of the International Neuropsychological Society (2016), **22**, 744–754.

doi:10.1017/S135561771600059X

Three-Dimensional Face Recognition in Mild Cognitive Impairment: A Psychophysical and Structural MR Study

Raquel Lemos,[1,2] Isabel Santana,[3] Gina Caetano,[1] Inês Bernardino,[1] Ricardo Morais,[4] Reza Farivar,[5,6] AND Miguel Castelo-Branco[1]

[1]Visual Neuroscience Laboratory, Institute of Biomedical Imaging and Life Sciences (CNC.IBILI), IBILI, Faculty of Medicine, University of Coimbra, Coimbra, Portugal
[2]Faculty of Psychology and Educational Sciences, University of Coimbra, Coimbra, Portugal
[3]Neurology Department of the Centro Hospitalar Universitário de Coimbra, Coimbra, Portugal
[4]Neuroradiology Department of the Centro Hospitalar Universitário de Coimbra, Coimbra, Portugal
[5]Harvard Medical School and Massachusetts General Hospital, A. Athinoula Martinos Center for Biomedical Imaging, Charlestown, Massachusetts
[6]McGill Vision Research, McGill University, Montreal, Canada

(Received July 28, 2015; Final Revision April 21, 2016; Accepted June 6, 2016)

Abstract

Objectives: Mild cognitive impairment (MCI) has been associated with a high risk of conversion to Alzheimer's dementia. In addition to memory complaints, impairments in the visuospatial domain have been reported in this condition. We have previously shown that deficits in perceiving structure-from-motion (SFM) objects are reflected in functional reorganization of brain activity within the visual ventral stream. Here we aimed to identify structural correlates of psychophysical complex face and object recognition performance in amnestic MCI patients ($n = 30$ *vs.* $n = 25$ controls). This study was, therefore, motivated by evidence from recent studies showing that a combination of visual information across dorsal and ventral visual streams may be needed for the perception of three-dimensional (3D) SFM objects. **Methods:** In our experimental paradigm, participants had to discriminate 3D SFM shapes (faces and objects) from 3D SFM meaningless (scrambled) shapes. **Results:** Morphometric analysis established neuroanatomical evidence for impairment in MCI as demonstrated by smaller hippocampal volumes. We found association between cortical thickness and face recognition performance, comprising the occipital lobe and visual ventral stream fusiform regions (overlapping the known location of face fusiform area) in the right hemisphere, in MCI. **Conclusions:** We conclude that impairment of 3D visual integration exists at the MCI stage involving also the visual ventral stream and contributing to face recognition deficits. The specificity of such observed structure-function correlation for faces suggests a special role of this processing pathway in health and disease. (*JINS*, 2016, *22*, 744–754)

Keywords: Mild cognitive impairment, Cortical thickness, Vision, Fusiform, Dorsal pathway, Ventral pathway, Structure-from-motion

INTRODUCTION

The clinical interest in predicting progression of cognitive impairment to dementia (particularly Alzheimer's disease, AD) has led to the definition of a transition period between normal cognitive function and dementia. This period has been defined using various clinical syndromal terms such as mild cognitive impairment (MCI) (Petersen et al., 1999), prodromal AD (Dubois et al., 2010, 2007), and "MCI due to AD" (Albert et al., 2011).

Correspondence and reprint requests to: Miguel Castelo-Branco, Visual Neuroscience Laboratory, IBILI-Faculty of Medicine, University of Coimbra, Azinhaga de Santa Comba, 3000-354 Coimbra, Portugal. E-mail: mcbranco@ibili.uc.pt

In addition to the expected episodic memory deficit, other brain systems may be altered in the preclinical (predementia) phases of AD, including visual function. Distinct forms of visual impairment have been extensively reported in AD, ranging from contrast sensitivity and color perception deficits to impairments in higher-order visual functions, including object and face perception and visual attention, as well as visual memory and learning (Butter, Trobe, Foster, & Berent, 1996; Duffy, Tetewsky, & O'Brien, 2000; Rizzo, Anderson, Dawson, & Nawrot, 2000). The prevalence of visual deficits is high in AD, with impairments found in a wide range of visual functions, suggesting a high vulnerability of pattern vision (52–59%), moderate vulnerability of spatial vision (20–33%), and low vulnerability (≤7%) of motion and flicker

perception in AD (Mendola, Cronin-Golomb, Corkin, & Growdon, 1995).

These findings suggest a dual compromise of the ventral visual pathway (Cronin-Golomb, 2004; Rizzo et al., 2000) and the dorsal stream (Bokde et al., 2010; Kavcic, Vaughn, & Duffy, 2011; Lemos, Figueiredo, Santana, Simoes, & Castelo-Branco, 2012) in AD. Research of visual function in MCI has mostly addressed high-level visual functions, showing in particular impairment in attentional and visual search tasks (Levinoff, Saumier, & Chertkow, 2005; Perry & Hodges, 2003; Tales, Haworth, Nelson, Snowden, & Wilcock, 2005). The literature available on low-level visual functions is scarce. However, Risacher et al. (2013) proved an early deficit in contrast sensitivity to be present in amnestic MCI patients, while Mapstone, Steffenella, and Duffy (2003) showed an impairment of radial motion detection in MCI subjects.

Most of the evidence concerning object perception in MCI comes from neuroimaging studies, showing in general patterns of decreased activation rather than directly measuring behavioral performance. Nevertheless, in a previous study, we found a selective deficit regarding integration of local motion cues into three-dimensional (3D) objects [structure-from-motion (SFM) stimuli] in a MCI group (Lemos et al., 2012). This study suggested a reorganization of ventral visual processing.

Motion processing involves multiple hierarchical steps, ranging from the magnocellular pathway, sensitive to high temporal frequency modulations, to subsequent motion integration within the visual cortical dorsal stream. To address motion processing, stimuli related to the perception of coherent two-dimensional (2D) patterns or 3D object structures derived from motion cues have been designed. The integration of the local motion cues to extract the 3D global configuration enables the perception of SFM stimuli. Thus, the standard stimuli used in SFM paradigms consist of physically coherent motion on a screen that produces a vivid illusion of a 3D object moving/rotating in depth.

Motion coherence paradigms have classically been used to address dorsal stream function, as validated by single unit studies in monkeys as well as functional imaging in humans (Braddick, O'Brien, Wattam-Bell, Atkinson, & Turner, 2000; Castelo-Branco et al., 2002, 2009; Orban, Sunaert, Todd, Van Hecke, & Marchal, 1999). These studies indicate that detection of motion coherence relies, at least partially, on a dedicated brain area in the dorsal stream [MT (middle temporal) in monkeys, and area V5 in humans] independently of earlier level magnocellular processing (Castelo-Branco et al., 2009). Early evidence from primate studies reported strong tuning in visual area MT for motion gradient selective neurons (Xiao, Marcar, Raiguel, & Orban, 1997), suggesting that the center-surround structure may support 3D slant and curvature perception. Mysore, Vogels, Raiguel, Todd, and Orban (2010) showed the selectivity of neurons of the fundus of the superior temporal sulcus (FST) for stimuli depicting specific shapes, coding motion-defined 3D shape fragments and underscoring the central role of FST in processing 3D-SFM. Moreover, although V5/MT lies along the dorsal stream, it has extensive connections with the ventral stream, which is consistent with the notion that motion processing involves multiple distributed pathways (Castelo-Branco et al., 2006; Mendes et al., 2005).

Accordingly, the neural correlates of SFM perception involve the integration of two main visual cortical pathways: the ventral stream underlying the recognition of object shape properties and the dorsal pathway involved in spatial vision and motion perception (Farivar, Blanke, & Chaudhuri, 2009; Konen & Kastner, 2008; Milner & Goodale, 2008).

Of interest, the neural substrates of SFM perception in MCI patients were found to predominantly relate to aberrant patterns of activation in fusiform face area/occipital face area (FFA/OFA) in the presence of normal recruitment of motion selective areas, suggesting the activation pattern within the ventral visual stream as a putative biomarker for MCI (Graewe et al., 2013). The study of visuospatial perception in the MCI group using an experimental paradigm requiring integration of dorsal and ventral processing may be important to clarify the role of these two visual pathways in the prediction of AD and better understand its pathophysiology, in addition to medial temporal lobe areas already known to be affected in this disorder (Jacobs et al., 2012; McKee et al., 2006; Villain, Chetelat, Desgranges, & Eustache, 2010; Villain, Fouquet, et al., 2010).

Previous functional magnetic resonance imaging (fMRI) studies suggested that reorganization may occur in both streams (Bokde et al., 2006; Prvulovic et al., 2002; Teipel et al., 2007; Vannini, Almkvist, Dierks, Lehmann, & Wahlund, 2007; Yamasaki, Muranaka, Kaseda, Mimori, & Tobimatsu, 2012).

The main goal of this study was to identify the structural correlates of the previously observed (Graewe et al., 2013; Lemos et al., 2012) deficits in complex face and object recognition, in MCI patients, and explore the contribution of both ventral and dorsal visual areas as putative biomarker of AD symptomatology. Our approach included a behavioral experimental paradigm with 3D SFM defined faces and objects and morphometric analysis comprising the computation of cortical thickness maps and hippocampal volumetry using MRI. We used SFM stimuli in which motion integration mechanisms in the dorsal stream form the basis for object recognition in the ventral stream. These stimuli, apart from probing dorsal–ventral integration provide an additional window on temporal lobe processes related to face perception in MCI (Graewe et al., 2013). In sum, this study aimed to investigate visual cortical structure-function relationships in 3D motion integration tasks, with a focus on changes in dorsal *versus* visual ventral pathways.

METHODS

Subjects

MCI patients ($n = 30$) were recruited from the Neurology Department of the Coimbra University Hospital. Diagnosis was reached through gold standard neurological and neuropsychological assessment following published classification criteria for MCI (Albert et al., 2011; Petersen, 2004).

https://doi.org/10.1017/S135561771600059X Published online by Cambridge University Press

All patients were of the amnestic "single domain" MCI type (at high risk for AD). Diagnostic investigation included a standard clinical evaluation, a staging assessment as well as laboratory tests including apolipoprotein E allele genotyping and imaging studies [MRI and single photon emission computed tomography/computed tomography (CT)].

The neuropsychological evaluation included a comprehensive diagnostic battery: (1) Cognitive instruments as the Mini-Mental State Examination (MMSE) (Folstein, Folstein, & McHugh, 1975) Portuguese version (Guerreiro, Silva, et al., 2008), the Alzheimer Disease Assessment Scale-Cognitive (ADAS-Cog) (Mohs, Rosen, & Davis, 1983) Portuguese version (Guerreiro, Fonseca, Barreto, & Garcia, 2008), and a comprehensive neuropsychological battery with normative data for the Portuguese population (BLAD) (Guerreiro, 1998) exploring learning and memory (Wechsler Memory Scale-R sub-tests: logical memory, verbal paired associative learning, and visual memory) and other cognitive domains: attention (cancelation task); verbal, motor, and graphomotor initiatives (verbal semantic fluency, motor and graphomotor initiative – Luria sequences); verbal comprehension (modified version of the Token test); sentences repetition; verbal and non-verbal abstraction (interpretation of proverbs and the Raven Progressive Matrices); visuoconstructional abilities; calculation (basic written calculation); immediate memory (Digit Span forward); working memory (Digit Span backward); right–left orientation and praxis (data not shown); (2) The Clinical Dementia Rating (CDR) (Morris, 1993) Portuguese version (Garrett et al., 2008) was used for global staging.

The inclusion criteria for MCI were those proposed by Petersen for MCI (Petersen, 2004; Petersen et al., 2001) and were operationalized as follows: (1) A subjective complaint of memory decline (reported by the subject or an informant); (2) An objective memory impairment (considered when scores on standard Wechsler memory tests were 1.5 standard deviation (*SD*) below age/education adjusted norms); (3) Normal general cognition suggested by normal scores in the MMSE and ADAS-Cog using the Portuguese cutoff scores (Guerreiro, Fonseca, et al., 2008; Guerreiro, Silva, et al., 2008); (4) Largely normal daily life activities; (5) Absence of dementia, indicated by a CDR rating of 0.5 (Morris, 1993).

Patients were excluded if they had other psychiatric or neurological conditions than MCI; CT or MRI demonstration of significant vascular burden (Roman et al., 1993) (large cortico-subcortical infarction; extensive subcortical white matter lesions superior to 25%; uni- or bilateral thalamic lacunae; lacunae in head of caudate nucleus; more than two lacunae). Furthermore, the exclusion of patients with significant vascular burden allowed us to ensure that our findings are due to AD pathology rather than vascular dementia.

Control participants ($n = 25$) were recruited among the patients' spouses, and age-matched hospital or university staff's relatives; with no relevant history of neurological or psychiatric conditions. All control participants had normal MMSE scores (mean 29.3; range, 27–30), absence of cognitive complaints and were independently functioning members of the community.

All participants had no history of abnormal ophthalmological conditions and had normal or corrected-to-normal vision.

Informed consent was obtained from all participants, and the study was conducted in accordance with the tenets of the Declaration of Helsinki, with the approval of our local ethics committee.

The two groups were matched for age [$t(53) = -1.149$; $p = .256$; d = 0.310], education levels [$U = 302$; $p = .204$; $\eta^2 = .029$], and sex [$\chi^2(1) = .039$; $p = .843$; $\varphi = 0.027$]. As expected MCI patients scored significantly lower on the MMSE than controls [$U = 257$; $p = .039$; $\eta^2 = .078$]. Demographical and clinical characteristics of the population are shown in Table 1.

Stimuli

The paradigm used in this study is based on the study of Graewe et al. (2013), in which participants had to discriminate between 3D SFM defined faces and scrambled

Table 1. Demographical and clinical characteristics of the population

	Control subjects ($n = 25$)	MCI ($n = 30$)	p	Effect size
Sex (m:f)	11:14	14:16	0.843	$\Phi = 0.027$
Age (years)	63.4 (1.7)	66.1 (1.5)	0.256	d = 0.310
Education level (years)	8.5 (0.7)	7.5 (0.8)	0.204	r = 0.171
MMSE (score)	29.3 (0.2)	28.5 (0.3)	0.039*	r = 0.279
CDR (score)	—	0.5 (0.0)	—	—
ApoE ε4 carrier, n (%)[a]	—	11 (36.7)	—	—
Positive family history, n (%)[b]	—	20 (66.7)	—	—

Note. Data are expressed as mean (SEM).
MCI = mild cognitive impairment; MMSE = Mini-Mental State Examination; CDR = Clinical Dementia Rating; d = Cohen's d effect size; φ = Phi effect size; r = Pearson *r* effect size for Mann-Whitney's U test.
[a]DNA was isolated from whole blood using a commercial kit (Roche Diagnostics GmbH, Manheim, Germany), as described by the manufacturer. ApoE genotype was determined by polymerase chain reaction-restriction fragment length polymorphisms (PCR-FLP) assay. No differences were found between ApoE ε4 carriers and non-carriers [$\chi^2(1) = 2.133$, $p = .144$].
[b]Among the group of ApoE ε4 carriers, 73% of subjects have a positive family history.
*$p < .05$.

https://doi.org/10.1017/S135561771600059X Published online by Cambridge University Press

shapes that were shown at three different durations (980 ms, 160 ms, and 100 ms). Nevertheless, in our study, only the intermediate duration condition (160 ms) was used as it was the only one capable of discriminating MCI patients from healthy elderly controls. Videos of 3D SFM defined faces (for details see Farivar et al., 2009), scrambled faces, chairs, and scrambled chairs were used as stimuli.

The face stimulus consisted of one laser-scanned facial surface taken from the Max-Planck Face Database (Troje & Bulthoff, 1996). The surfaces were rendered into a volumetric texture map to ensure uniform texture density, a process analogous to carving a surface out of a stone block. Shadows and shading were removed from the rendering. The faces were rendered against a similarly textured random-dot background. During the animation, the face rotated from –22.5 degrees to 22.5 degrees, centered at the frontal plan, in one cycle (Fig. 1a).

In the present study, we also included the chair stimulus which was obtained from a chair model database and was rendered in exactly the same manner as the face stimulus. Scrambled versions of the two stimuli were constructed by cutting the rendered whole object (face or chair) videos on the horizontal plane into 10 blocks and scrambling their local curvatures/positions. The resulting scrambled stimuli share many of the low-level features of the original videos and are recognized as unfamiliar objects. It is important to note that these motion-defined objects are only visible when the animation is playing; otherwise participants are not able to interpret the SFM cues to extract a vivid 3D percept, as desired.

Stimulus depth information was parametrically manipulated at three different levels resulting in an overall 4 (stimulus category) × 3 (depth levels) design. The depth manipulation was included with the purpose of increasing the task complexity and unpredictability at variable 3D levels. The different depth levels created (full, intermediate, and flat) were, however, not intended as main outcome measures. They were, therefore, pooled for the purposes of this study (Fig. 1b). Ten trials per parameter value were included, in a total of 120 trials (Fig. 1c).

Procedure

Participants were individually tested in a quiet and darkened room. They were seated in a comfortable chair at a distance of 50 cm from the computer screen. The stimuli, subtending ~13° horizontally and ~10° vertically, were presented in the center of a 33.8 cm × 27.1 cm dark computer screen (1280 × 1024 pixels) using the software package Presentation (Neurobehavioral systems).

Participants had to discriminate 3D SFM objects (faces and chairs) from 3D SFM meaningless objects (scrambled faces and scrambled chairs) on videos of 160 ms duration. The tasks were subdivided in a Chair discrimination task and a Face discrimination task in which participants had to report if the presented stimulus was upright or scrambled. The investigator recorded participants' verbal responses using a 2-button response box to exclude confounding factors such as motor errors. The verbal instruction was the same for all participants and was as follows: "In this computer screen it will be briefly shown a video of a face (or chair) or a scrambled version of that face (or chair). You should look attentively and say if an upright or a scrambled face (or chair) was presented. After the video disappearance the screen will be black, and after your response another video will appear".

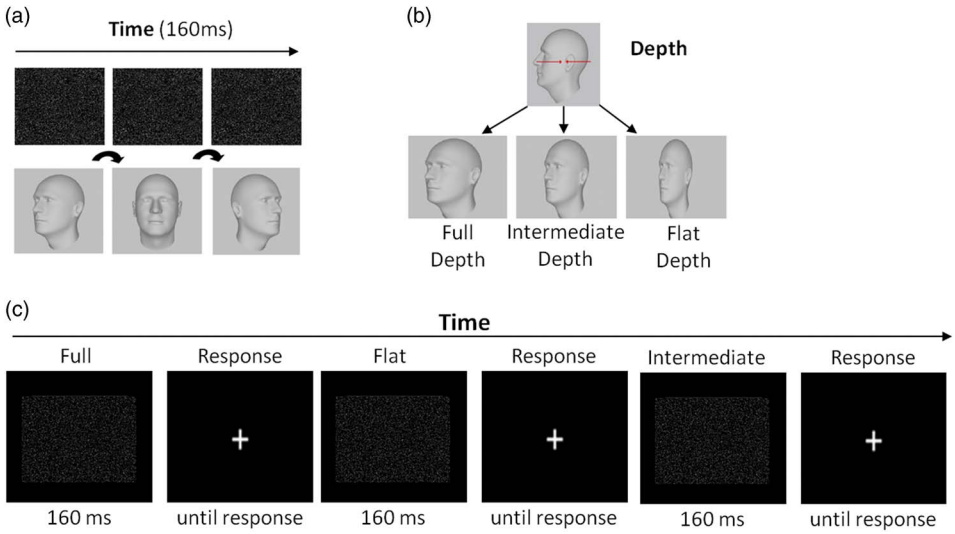

Fig. 1. Stimuli and paradigm (adapted from Graewe et al., 2013) (**a**) SFM faces rotated from left to right in one cycle and were shown during 160 ms. Object perception is rendered possible by integration of the moving dot pattern, the object being physically absent when the rotation/motion is absent; (**b**) The depth modulation resulted in SFM stimulus conditions with variable depth levels parameterized in terms of anterior–posterior range; (**c**) Stimuli were presented randomly at one of the three depth levels, separated by a fixation period during which the participants had unlimited time for response. The images of the heads included in the figure just illustrate the structure in the SFM stimuli and do not represent (because they are physically absent and not visible in static images) the exact percept constructed during the movies' presentation.

https://doi.org/10.1017/S135561771600059X Published online by Cambridge University Press

Before performing the experimental tasks, all participants underwent a demonstration and a practice phase. In the demonstration phase, the stimuli included in both Face and Chair tasks were shown to allow the participants to become familiar with the objects that they would be asked to recognize afterward. Three learning trials were administered for each task condition. The practice phase was repeated whenever the participant did not understand the instructions.

Image (MRI) Acquisition

Participants underwent MRI scanning on a 3 Tesla (T) Siemens Magnetom Trio scanner (Erlangen, Germany), using a 12-channel birdcage head coil. All participants belong to a local MRI cohort database, comprising a total of 108 MCI and 76 controls, from which 30 MCI and 18 controls participated in the psychophysics experiment described in the above section.

One (and often two) high-resolution 3D T1-weighted magnetization-prepared rapid gradient echo (MP-RAGE) scans were collected per participant, with parameters defined on the basis of guidelines from the Alzheimer's Disease Network Initiative (ADNI) (Jack et al., 2008): field of view = 256, 160 slices, voxel resolution $1 \times 1 \times 1$ mm^3, repetition time = 2300 ms, echo time = 2.98 ms, inversion time = 900 ms, 9° flip angle, bandwidth 240 Hz/px, acceleration factor of 2 with 24 reference lines in the phase encoding direction. Acquisition parameters were optimized for increased gray-white matter image contrast, while minimizing acquisition time.

Image Analysis Procedures

Measurement of cortical thickness and volumes in individual participants

The structural MRI scans were processed with the FreeSurfer 5.0.0 software package (http://surfer.nmr.mgh.harvard.edu) using methods that are fully automated and extensively described (Dale, Fischl, & Sereno, 1999; Desikan et al., 2006; Fischl & Dale, 2000; Fischl et al., 2002, 2004; Fischl, Sereno, & Dale, 1999; Han et al., 2006). Each magnetization-prepared rapid gradient-echo (MPRAGE) MRI acquisition image was visually inspected for abnormalities unrelated to the underlying pathology, such as movement artifacts or concomitant pathologies. When available, two MRI acquisitions for each participant (n = 12/30 for the MCI group; n = 10/18 for the control group) were motion corrected, averaged and normalized for intensity inhomogeneities, resulting on a single image. The resulting volume was used to locate the gray/white matter boundary, then used as a starting point to define the gray/cerebrospinal fluid boundary across the entire cortical mantle.

For each participant, cortical thickness was estimated at each point of the cortical mantle by finding the shortest distance from the white matter surface to the gray matter surface (and *vice-versa*) and averaging those two values (Fischl & Dale, 2000). The neocortex was parcellated onto 32 gyral-based regions-of-interest (ROI) (Fischl et al., 2002, 2004), in each hemisphere, and in addition non-neocortical ROIs, such as the hippocampus, were defined on the basis of automated procedures (Desikan et al., 2006). The neocortex automated atlas-based parcellation was used for labeling purposes in later cortical thickness data analysis stages.

For each participant, the accuracy of the gray and white matter surfaces and of each individual ROI was carefully inspected by a trained neuroradiologist. When necessary, manual editing and corrections were applied, precluding skull stripping, white matter, control points, and removing inclusion of dura matter in gray matter surface (http://surfer.nmr.mgh.harvard.edu/fswiki/FsTutorial/).

Registration and group cortical thickness maps

For each participant, the white matter surface was morphed to an average spherical surface folding pattern representation (this was performed one hemisphere at a time) from which surface maps of cortical thickness were generated, at each vertex of the cortical mantle (Fischl et al., 1999). Smoothing of the data on the cortical tessellation was performed with a 2D surface-based Gaussian kernel of ≈20 mm full width half maximum (kernel sizes of 15 mm and 10 mm were also tested and the pattern of results did not change).

Data Analysis

Statistical analysis was performed with the SPSS statistical software package, version 19.0 (SPSS, Inc., Chicago, IL) with parametric and non-parametric tests (used when data significantly deviated from normal distributions, verified using the Kolmogorov-Smirnov normality check and Levene homogeneity tests), corrected for multiple comparisons, when applicable. Results with $p < .05$ were considered statistically significant.

Psychophysics

For the statistical analysis of the behavioral data, a d' (dprime) performance measure [d' = Z(hit rate) – Z(false alarm rate)], as well as a response bias measure [c = –0.5[z (hit rate) + z(false alarm rate)]] were computed for face and chair detection for each participant. A hit was considered when the subject recognized correctly the stimulus, whereas a false alarm was considered for conditions when the subject reported face/chair detection in the presence of a scrambled stimulus. Mann-Whitney U tests were performed for comparison between the two groups.

Imaging

Hippocampal volumes

Two non-neocortical ROIs, left and right hemispheres' hippocampi, were used in this study with the purpose of assessing differences between MCI and control groups (independent samples t tests), in regions known to be pivotal

https://doi.org/10.1017/S135561771600059X Published online by Cambridge University Press

in AD pathology. Volume measures were normalized for differences in estimated total intracranial volume through a ratio procedure.

Cortical thickness and vertex-based correlational analysis

Analysis was performed using the cortical thickness maps obtained through spherical mapping and smoothing. A vertex-by-vertex analysis was carried out using a general linear model, with cortical thickness as the dependent variable and group as the independent variable. Age interaction effects were considered, and the number of structural MR images was introduced as a nuisance factor. Correction for multiple comparisons was applied using false discovery rate (FDR) at a .05 significance level.

Correlational analysis was performed, on a vertex-by-vertex basis, regressing cortical thickness against behavioral performance measures (dprime), and nuisance factors were taken into account, with the inclusion of participants' age and the number of structural images per participant. Again, correction for multiple comparisons was applied using FDR at a .05 significance level. The ROI clusters that survived FDR correction were delineated separately, and the corresponding value for mean cortical thickness was calculated for each of the MCI participants. To further examine the association between the ROI clusters' mean cortical thickness and face recognition performance, spearman correlation coefficients were calculated. Additionally, hierarchical multiple regression was performed to account for the role of chronological age as a putative confound factor. Results were analyzed in terms of R^2 and analysis of variance table for multiple regression, and also the coefficients table whenever previous results were statistically significant at a 5% significance level. Hierarchical multiple regressions were performed separately for the control and MCI group.

RESULTS

A Mann-Whitney test for the dprime values indicated that the MCI group ($M = 1.78$; $SD = 1.27$) performed significantly worse than the control group ($M = 2.72$; $SD = 1.54$) regarding face recognition ($U = 211.5$; $p = .006$; $\eta^2 = .138$). Performance differences were also found for the chairs category ($U = 236$; $p = .016$; $\eta^2 = .105$) with participants with MCI ($M = 5.97$; $SD = 2.40$) exhibiting more difficulties than control participants ($M = 7.56$; $SD = 2.31$) in distinguishing between 3D SFM chairs and 3D SFM meaningless shapes (Fig. 2). Response bias analyses revealed no significant differences between the groups, both for face ($U = 430.0$; $p = .352$; $\eta^2 = .016$) and chairs conditions ($U = 422.0$; $p = .422$; $\eta^2 = .012$). Accuracy measures revealed that both groups showed a higher performance level for the chairs category (MCI: $M = .961$; $SD = .050$; Controls: $M = .989$; $SD = .021$) than for the face recognition condition (MCI: $M = .732$; $SD = .169$; Controls: $M = .855$; $SD = .108$).

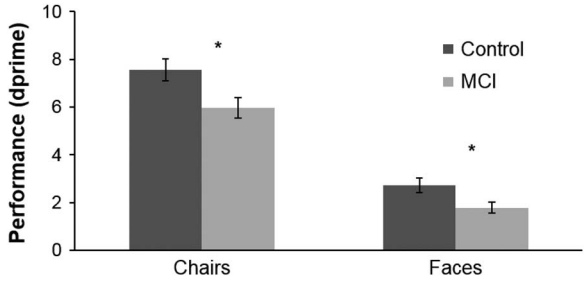

Fig. 2. Performance (as assessed by dprime measures) for the global Face and Chair Conditions. Stimulus duration: 160 ms. *significant difference (for exact p values see text).

Hippocampal Volumetry, Cortical Thickness, and Vertex-Based Correlational Analysis

Hippocampal volumes were smaller, bilaterally, in the MCI group (right: $M = 2.47$; $SD = 0.35$; left: $M = 2.28$; $SD = 0.36$), compared to control participants (right: $M = 2.69$; $SD = 0.34$; left: $M = 2.61$; $SD = 0.34$) reaching statistical significance for both right ($t(46) = 2.089$; $p < .05$; $d = 0.638$) and left ($t(46) = 3.117$; $p < .01$; $d = 0.942$) hemispheres (analysis performed independently for each hemisphere). On the other hand, no statistically significant differences in cortical thickness were observed between MCI and control groups.

Correlational analysis unveiled significant results for the MCI group, whereas similar findings were not observed for the control group. Significant correlations between cortical thickness and behavioral measures, for the MCI group, are depicted in Figure 3 (corrected for multiple comparisons; q(FDR) of 0.05). Positive associations of cortical thickness and the face recognition performance (as assessed by dprime values), for the right hemisphere (in line with the known right hemispheric lateralization for face recognition), were identified in the MCI group, comprising occipital lobe (BA18; $\rho = 0.583$; $p < .0005$) and fusiform (BA37; $\rho = 0.320$; $p < .05$) regions (Table 2, showing a region overlapping FFA as identified by Graewe et al. 2013) involved in visual face processing. No significant correlations applied for the chairs condition.

To explore the impact of chronological age in this associations, a hierarchical multiple regression was performed applying the Enter method, using age and either cortical thickness of BA18 area or cortical thickness of BA37 area as independent variables for predicting the performance on face discrimination task.

Regarding the BA18 area, for the MCI group, and despite an inexistent statistically significant impact of age ($R^2 = 0.115$; $F(1,28) = 3.632$; $p = .067$), when it is considered combined with cortical thickness measure, both variables explain approximately 66% of the variability of the performance in the face discrimination ($R^2 = 0.660$; $F(2,27) = 26.22$; $p < .001$). Both variables present statistically significant coefficients, although greater importance can be ascribed to cortical thickness ($b = 4.485 + 0.682$; $p < .001$) than to age ($b = -0.044 + 0.018$; $p = .020$). Notice that performance on face discrimination condition

https://doi.org/10.1017/S135561771600059X Published online by Cambridge University Press

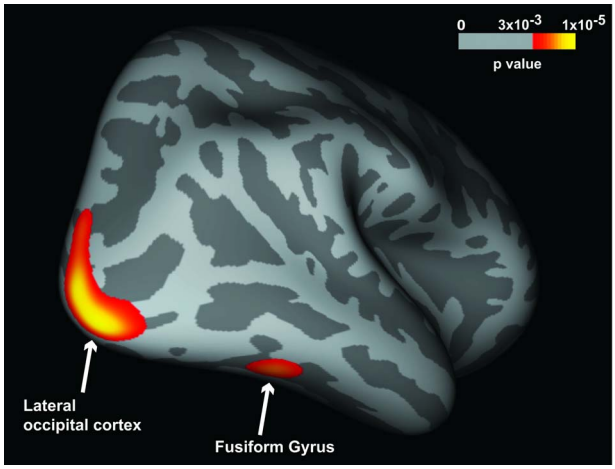

Fig. 3. Statistical results rendered on an inflated gray matter surface. The cortical areas in which thickness positively correlates with dprime scores (see Table 2) are depicted. The color scale represents the p values as depicted for significant correlations (corrected for multiple comparisons: FDR at .05 significance level).

decreases with the decrease of cortical thickness in the BA18 area and the increase of age.

The same pattern was found concerning the BA37 area. In the MCI group, and despite an inexistent statistically significant impact of age ($R^2 = 0.115$; $F(1,28) = 3.632$; $p = .067$, as explained above), when it is considered combined with the cortical thickness measure, both variables explain approximately 48% of the variability found in the performance of face discrimination task ($R^2 = 0.482$; $F(2,27) = 12.583$; $p < .001$). Both variables present statistically significant coefficients for predicting face discrimination, although, once again, greater importance can be ascribed to the cortical thickness ($b = 2.279 + 0.520$; $p < .001$) than to age ($b = -0.068 + 0.022$; $p = .005$). Performance on face discrimination task decreases with the decrease of cortical thickness in the BA37 area and the increase of age.

For the control group, we did not find any statistically significant impact of age, for itself, in changes in the performance in the face discrimination task.

Globally, face discrimination abilities seem to be associated with cortical thickness measures of both BA18 and BA37 areas, when age is considered as covariate, in MCI patients, but not in controls.

DISCUSSION

Here, we investigated the structural correlates of visual integration of 3D SFM face/objects, in MCI. Our paradigm requires visual integration across features, which involves dorsal stream motion coherence extraction, before visual ventral stream processing of object features (Farivar et al., 2009; Graewe et al., 2013). We had already established before that 2D and 3D motion integration is particularly deteriorated during normal and pathological ageing independently of lower level deficits (Castelo-Branco et al., 2009; Graewe et al., 2013; Mateus et al., 2009)

Behavioral results confirmed that high level integration in visual face recognition is impaired in MCI, thereby extending previous results on coherence thresholds of simple spherical objects (Lemos et al., 2012). Temporal requirements for visual integration were chosen (160 ms) to impose a performance challenge. We found an association of task performance with ventral stream integrity, suggesting that this pathway becomes a limiting step for performance in MCI.

While not excluding an important role for dorsal stream processing that was found in previous studies, the present results suggest that the ventral pathway also plays an important role, as demonstrated here for face stimuli, concerning whole brain structure-function correlation analyses. Indeed, the patients with larger fusiform cortical thickness had more preserved recognition performance, but only for faces and not chairs. These results do not dispute the notion that the dorsal stream is also affected as suggested by the work of Rizzo et al. (2000) on motion perception and our own previous imaging and psychophysical studies (Graewe et al., 2013; Lemos et al., 2012).

Although the main finding of this study is the observed structural functional correlations for faces, we cannot exclude that chair recognition might also be related to structural changes. Although chair recognition was also impaired, it is possible that the relatively higher performance levels precluded the identification of a structural correlate. Another novelty of our study is the report of visual structure-function correlations at the stage of MCI, as the majority of imaging studies on AD-related pathology have documented structural/functional changes of regions related with the memory impairment, such as the hippocampus and related structures in the medial temporal lobe (Albert et al., 2011; Dubois et al., 2010, 2007; Sperling, 2011; Teipel et al., 2013). Nonetheless, previous studies have suggested that visual responses are

Table 2. Cortical areas showing positive correlations between thickness and psychophysical dprime scores in the MCI group in the face integration condition that differentiates between groups

	BA	Hemisphere	Area	*p*-Value	Talairach Coordinatescoordinates	Spearman ρ	p-*Value*
Occipital Lobelobe	BA18	R	1329	<.00005	25, −95, −2	0.583	<.0005
Fusiform	BA37	R	163	<.0001	41, −53, −7	0.320	<.05

Note. p-Values are reported at the vertex maxima for each cluster, and respective Talairach coordinates were estimated on basis of non-linear MNI to Talairach transformation (white matter surface). The fusiform cluster overlaps the previously described Fusiform Face Area region (Graewe et al., 2013). Spearman correlation coefficients (one-tailed) were estimated for the mean cortical thickness, of each significant cluster, and the dprime face recognition performance. BA = Broadmann area; Area = cluster surface area in mm^2.

https://doi.org/10.1017/S135561771600059X Published online by Cambridge University Press

modified in MCI and AD (Bokde et al., 2006; Mentis et al., 1996; Prvulovic et al., 2002; Teipel et al., 2007; Vannini et al., 2007; Yamasaki et al., 2012). However, it has remained difficult to establish a direct correlation with performance.

In our study, we found that behavioral performance is significantly correlated with cortical thickness. Accordingly, after controlling for different nuisance factors, we found significantly positive correlations with face recognition condition and thickness in both the occipital lobe (BA18), and the ventral fusiform (BA37) areas on the right hemisphere, in the MCI group. These correlations were found in the condition that was previously reported (Graewe et al., 2013) to better discriminate MCI patients from healthy elderly and corroborated in the present study. Some psychophysical studies had indicated that the ventral visual pathway is more affected in AD spectrum (Cronin-Golomb, 2004; Rizzo et al., 2000) although, as stated above, this does not exclude afferent dorsal stream deficits (Bokde et al., 2010; Kavcic et al., 2011; Lemos et al., 2012).

The lack of cortical differences in the control group, as function of face recognition performance, suggest a disease specific mechanism. The positive associations of cortical thickness and face recognition performance identified in the MCI group suggest that the larger the amount of gray matter in this region, the higher the performance levels. This might suggest that the level of integrity of the visual ventral pathway is critical for object recognition in MCI. These findings are also consistent with the Scaffolding Theory of Aging and Cognition, which represents the brain as a dynamically adaptive structure that changes in both positive and negative ways with age (Reuter-Lorenz & Park, 2014).

Our results confirm the tenet that the fusiform gyrus (BA37), comprising the fusiform face area, may be critically affected in distinct stages of the natural history of AD (Bokde et al., 2006; Graewe et al., 2013; Teipel et al., 2007). Furthermore, our findings do suggest that the right BA37 is more closely associated with performance changes which is also consistent with the notion of lateralization of face-selective responses in the right hemisphere (for a review, see Cabeza & Nyberg, 2000). Moreover, the findings from the present work, corroborate the previous findings of Graewe et al. (2013) on the decreased sensitivity for faces in the right FFA, in MCI patients. The fusiform region identified in this study overlaps the FFA region described in that study. The involvement of extrastriate visual cortex may help explain the early visual deficits in AD-related pathology found by other groups (Risacher et al., 2013; Rizzo et al., 2000; Rose et al., 2006). The finding that the ventral pathway is important for SFM perception is consistent with the idea that ventral processing is also required for visual integration (James, Humphrey, Gati, Menon, & Goodale, 2002; Klaver et al., 2008; Orban et al., 1999).

Our study also suggests new ways of studying complex object recognition (in particular face processing) and its neural correlates in pathological ageing. Dynamic aspects of a visual scene provide important cues for object segregation and identification, and 3D SFM paradigms are particularly relevant in this context. Dynamic cues are highly informative of an object's shape and may be capable of driving complex recognition processes in the absence of other shape cues. The visual integration ability needed to achieve holistic perception of the whole 3D shape from local information seems to be impaired in MCI patients, and to also require the ventral pathway. Our results suggest the existence of important nodes within the ventral pathway that provide a substrate for 3D object processing in MCI.

In sum, we found evidence for a strong correlation between recognition of complex 3D moving faces and integrity in extrastriate and a fusiform region overlapping FFA in MCI.

ACKNOWLEDGMENTS

Authors thank all the participants. Authors also thank Carlos Ferreira and João Marques for help with MRI scanning, as well as Francisco Caramelo and João Pereira for help with statistical analysis. None of the authors have any conflict of interest related to this work. This work was supported by grants from the Foundation for Science and Technology Portugal: SFRH/BD/74070/2010 (to R.L.); PIC/IC/83206/2007 (to I.S.); Programa Ciência 2008 and PTDC/SAU-ENB/112306/2009 (to G.C.); CENTRO-07-ST24-FEDER–00205, FCT- UID/NEU/04539/2013, and COMPETE, POCI-01-0145-FEDER-007440 (to M.C.B.).

REFERENCES

Albert, M.S., DeKosky, S.T., Dickson, D., Dubois, B., Feldman, H.H., Fox, N.C., … Phelps, C.H. (2011). The diagnosis of mild cognitive impairment due to Alzheimer's disease: Recommendations from the National Institute on Aging-Alzheimer's Association workgroups on diagnostic guidelines for Alzheimer's disease. *Alzheimer's & Dementia*, *7*, 270–279. doi:10.1016/j.jalz.2011.03.008

Bokde, A.L., Lopez-Bayo, P., Born, C., Ewers, M., Meindl, T., Teipel, S.J., … Hampel, H. (2010). Alzheimer disease: Functional abnormalities in the dorsal visual pathway. *Radiology*, *254*, 219–226. doi:10.1148/radiol.2541090558

Bokde, A.L., Lopez-Bayo, P., Meindl, T., Pechler, S., Born, C., Faltraco, F., … Hampel, H. (2006). Functional connectivity of the fusiform gyrus during a face-matching task in subjects with mild cognitive impairment. *Brain*, *129*(Pt 5), 1113–1124. doi:10.1093/brain/awl051

Braddick, O.J., O'Brien, J.M., Wattam-Bell, J., Atkinson, J., & Turner, R. (2000). Form and motion coherence activate independent, but not dorsal/ventral segregated, networks in the human brain. *Current Biololgy*, *10*, 731–734. doi:10.1016/S0960-9822(00)00540-6

Butter, C.M., Trobe, J.D., Foster, N.L., & Berent, S. (1996). Visual-spatial deficits explain visual symptoms in Alzheimer's disease. *American Journal of Ophthalmology*, *122*, 97–105. doi:10.1016/S0002-9394(14)71969-5

Cabeza, R., & Nyberg, L. (2000). Imaging cognition II: An empirical review of 275 PET and fMRI studies. *Journal of Cognitive Neuroscience*, *12*, 1–47. doi:10.1162/08989290051137585

Castelo-Branco, M., Formisano, E., Backes, W., Zanella, F., Neuenschwander, S., Singer, W., & Goebel, R. (2002). Activity patterns in human motion-sensitive areas depend on the

interpretation of global motion. *Proceedings of the National Academy of Sciences of the United States of America*, *99*, 13914–13919. doi:10.1073/pnas.202049999

Castelo-Branco, M., Mendes, M., Silva, F., Massano, J., Januario, G., Januario, C., … Freire, A. (2009). Motion integration deficits are independent of magnocellular impairment in Parkinson's disease. *Neuropsychologia*, *47*, 314–320. doi:10.1016/j.neuropsychologia.2008.09.003

Castelo-Branco, M., Mendes, M., Silva, M.F., Januario, C., Machado, E., Pinto, A., … Freire, A. (2006). Specific retinotopically based magnocellular impairment in a patient with medial visual dorsal stream damage. *Neuropsychologia*, *44*, 238–253. doi:10.1016/j.neuropsychologia.2005.05.005

Cronin-Golomb, A. (2004). Heterogeneity of visual presentation in Alzheimer's disease. In A. Cronin-Golomb & P.R. Hof (Eds.), *Vision in Alzheimer's disease* (*Vol. 34*, pp. 96–11). Switzerland: Karger.

Dale, A.M., Fischl, B., & Sereno, M.I. (1999). Cortical surface-based analysis. I. Segmentation and surface reconstruction. *Neuroimage*, *9*, 179–194. doi:10.1006/nimg.1998.0395

Desikan, R.S., Segonne, F., Fischl, B., Quinn, B.T., Dickerson, B.C., Blacker, D., … Killiany, R.J. (2006). An automated labeling system for subdividing the human cerebral cortex on MRI scans into gyral based regions of interest. *Neuroimage*, *31*, 968–980. doi:10.1016/j.neuroimage.2006.01.021

Dubois, B., Feldman, H.H., Jacova, C., Cummings, J.L., Dekosky, S.T., Barberger-Gateau, P., … Scheltens, P. (2010). Revising the definition of Alzheimer's disease: A new lexicon. *Lancet Neurology*, *9*, 1118–1127. doi:10.1016/S1474-4422(10)70223-4

Dubois, B., Feldman, H.H., Jacova, C., Dekosky, S.T., Barberger-Gateau, P., Cummings, J., … Scheltens, P. (2007). Research criteria for the diagnosis of Alzheimer's disease: Revising the NINCDS-ADRDA criteria. *Lancet Neurology*, *6*, 734–746. doi:10.1016/S1474-4422(07)70178-3

Duffy, C.J., Tetewsky, S.J., & O'Brien, H. (2000). Cortical motion blindness in visuospatial AD. *Neurobiology of Aging*, *21*, 867–869. doi:10.1016/S0197-4580(00)00187-1

Farivar, R., Blanke, O., & Chaudhuri, A. (2009). Dorsal-ventral integration in the recognition of motion-defined unfamiliar faces. *Journal of Neuroscience*, *29*, 5336–5342. doi:10.1523/JNEUROSCI.4978-08.2009

Fischl, B., & Dale, A.M. (2000). Measuring the thickness of the human cerebral cortex from magnetic resonance images. *Proceedings of the National Academy of Sciences of the United States of America*, *97*, 11050–11055. doi:10.1073/pnas.200033797

Fischl, B., Salat, D.H., Busa, E., Albert, M., Dieterich, M., Haselgrove, C., … Dale, A.M. (2002). Whole brain segmentation: Automated labeling of neuroanatomical structures in the human brain. *Neuron*, *33*, 341–355. doi:10.1016/S0896-6273(02)00569-X

Fischl, B., Sereno, M.I., & Dale, A.M. (1999). Cortical surface-based analysis. II: Inflation, flattening, and a surface-based coordinate system. *Neuroimage*, *9*, 195–207. doi:10.1006/nimg.1998.0396

Fischl, B., van der Kouwe, A., Destrieux, C., Halgren, E., Segonne, F., Salat, D.H., … Dale, A.M. (2004). Automatically parcellating the human cerebral cortex. *Cerebral Cortex*, *14*, 11–22. doi:10.1093/cercor/bhg087

Folstein, M.F., Folstein, S.E., & McHugh, P.R. (1975). "Mini-mental state". A practical method for grading the cognitive state of patients for the clinician. *Journal of Psychiatric Research*, *12*, 189–198. doi:10.1016/0022-3956(75)90026-6

Garrett, C., Santos, F., Tracana, I., Barreto, J., Sobral, M., & Fonseca, R. (2008). Avaliação clínica da demência [Clinical Dementia Rating]. In A. Mendonça, C. Garcia & M. Guerreiro (Eds.), *Escalas e testes de demência. [Scales and tests in dementia] Grupo de Estudos de Envelhecimento Cerebral e Demência* (pp. 18–32). Lisbon: GEECD.

Graewe, B., Lemos, R., Ferreira, C., Santana, I., Farivar, R., De Weerd, P., & Castelo-Branco, M. (2013). Impaired processing of 3D motion-defined faces in mild cognitive impairment and healthy aging: An fMRI study. *Cerebral Cortex*, *23*, 2489–2499. doi:10.1093/cercor/bhs246

Guerreiro, M. (1998). *Contributo da Neuropsicologia para o estudo das demências [Contribution of Neuropsychology to the study of dementia].* (Unpublished doctoral dissertation), University of Lisbon, Lisbon.

Guerreiro, M., Fonseca, S., Barreto, J., & Garcia, C. (2008). Escala de avaliação da doença de Alzheimer - EADA [Alzheimer Disease Assessment Scale- ADAS]. In A. Mendonça, C. Garcia, & M. Guerreiro (Eds.), *Escalas e testes de demência. [Scales and tests in dementia] Grupo de Estudos de Envelhecimento Cerebral e Demência* (pp. 42–58). Lisbon: GEECD.

Guerreiro, M., Silva, A.P., Botelho, M.A., Leitão, O., Castro-Caldas, A., & Garcia, C. (2008). Avaliação breve do estado mental [Mini Mental State Examination]. In A. Mendonça, C. Garcia, & M. Guerreiro (Eds.), *Escalas e testes de demência [Scales and tests in dementia] Grupo de Estudos de Envelhecimento Cerebral e Demência* (pp. 33–39). Lisbon: GEECD.

Han, X., Jovicich, J., Salat, D., van der Kouwe, A., Quinn, B., Czanner, S., … Fischl, B. (2006). Reliability of MRI-derived measurements of human cerebral cortical thickness: The effects of field strength, scanner upgrade and manufacturer. *Neuroimage*, *32*, 180–194. doi:10.1016/j.neuroimage.2006.02.051

Jack, C.R., Jr., Bernstein, M.A., Fox, N.C., Thompson, P., Alexander, G., Harvey, D., … Weiner, M.W. (2008). The Alzheimer's Disease Neuroimaging Initiative (ADNI): MRI methods. *Journal of Magnetic Resonance Imaging*, *27*, 685–691. doi:10.1002/jmri.21049

Jacobs, H.I., Gronenschild, E.H., Evers, E.A., Ramakers, I.H., Hofman, P.A., Backes, W.H., … Van Boxtel, M.P. (2012). Visuospatial processing in early Alzheimer's disease: A multimodal neuroimaging study. *Cortex*, *64*, 394–406. doi:10.1016/j.cortex.2012.01.005

James, T.W., Humphrey, G.K., Gati, J.S., Menon, R.S., & Goodale, M.A. (2002). Differential effects of viewpoint on object-driven activation in dorsal and ventral streams. *Neuron*, *35*, 793–801. doi:10.1016/S0896-6273(02)00803-6

Kavcic, V., Vaughn, W., & Duffy, C.J. (2011). Distinct visual motion processing impairments in aging and Alzheimer's disease. *Vision Research*, *51*, 386–395. doi:10.1016/j.visres.2010.12.004

Klaver, P., Lichtensteiger, J., Bucher, K., Dietrich, T., Loenneker, T., & Martin, E. (2008). Dorsal stream development in motion and structure-from-motion perception. *Neuroimage*, *39*, 1815–1823. doi:10.1016/j.neuroimage.2007.11.009

Konen, C.S., & Kastner, S. (2008). Two hierarchically organized neural systems for object information in human visual cortex. *Nature Neuroscience*, *11*, 224–231. doi:10.1038/nn2036

Lemos, R., Figueiredo, P., Santana, I., Simoes, M.R., & Castelo-Branco, M. (2012). Temporal integration of 3D coherent motion cues defining visual objects of unknown orientation is impaired in amnestic mild cognitive impairment and Alzheimer's disease. *Journal of Alzheimer's Disease*, *28*, 885–896. doi:10.3233/JAD-2011-110719

Levinoff, E.J., Saumier, D., & Chertkow, H. (2005). Focused attention deficits in patients with Alzheimer's disease and mild cognitive impairment. *Brain & Cognition*, *57*, 127–130. doi:10.1016/j.bandc.2004.08.058

Mapstone, M., Steffenella, T.M., & Duffy, C.J. (2003). A visuospatial variant of mild cognitive impairment: Getting lost between aging and AD. *Neurology*, *60*, 802–808. doi:10.1212/01.WNL.0000049471.76799.DE

Mateus, C., Lemos, R., Silva, M.F., Reis, A., Fonseca, P., Oliveiros, B., & Castelo-Branco, M. (2009). Aging of low and high level vision: From chromatic and achromatic contrast sensitivity to local and 3D object motion perception. *PLoS One*, *8*, 1–10. doi:10.1371/journal.pone.0055348

McKee, A.C., Au, R., Cabral, H.J., Kowall, N.W., Seshadri, S., Kubilus, C.A., … Wolf, P.A. (2006). Visual association pathology in preclinical Alzheimer disease. *Journal of Neuropathology and Experimental Neurology*, *65*, 621–630. doi:10.1097/00005072-200606000-00010

Mendes, M., Silva, F., Simoes, L., Jorge, M., Saraiva, J., & Castelo-Branco, M. (2005). Visual magnocellular and structure from motion perceptual deficits in a neurodevelopmental model of dorsal stream function. *Cognitive Brain Research*, *25*, 788–798. doi:10.1016/j.cogbrainres.2005.09.005

Mendola, J.D., Cronin-Golomb, A., Corkin, S., & Growdon, J.H. (1995). Prevalence of visual deficits in Alzheimer's disease. *Optometry and Vision Science*, *72*, 155–167. doi:10.1097/00006324-199503000-00003

Mentis, M.J., Horwitz, B., Grady, C.L., Alexander, G.E., VanMeter, J.W., Maisog, J.M., … Rapoport, S.I. (1996). Visual cortical dysfunction in Alzheimer's disease evaluated with a temporally graded "stress test" during PET. *American Journal of Psychiatry*, *153*, 32–40. doi:10.1176/ajp.153.1.32

Milner, A.D., & Goodale, M.A. (2008). Two visual systems re-viewed. *Neuropsychologia*, *46*, 774–785. doi:10.1016/j.neuropsychologia.2007.10.005

Mohs, R.C., Rosen, W.G., & Davis, K.L. (1983). The Alzheimer's disease assessment scale: An instrument for assessing treatment efficacy. *Psychopharmacology Bulletin*, *19*, 448–450.

Morris, J.C. (1993). The Clinical Dementia Rating (CDR): Current version and scoring rules. *Neurology*, *43*, 2412–2414. doi:10.1212/WNL.43.11.2412-a

Mysore, S.G., Vogels, R., Raiguel, S.E., Todd, J.T., & Orban, G.A. (2010). The selectivity of neurons in the macaque fundus of the superior temporal area for three-dimensional structure from motion. *Journal of Neuroscience*, *30*, 15491–15508. doi:10.1523/JNEUROSCI.0820-10.2010

Orban, G.A., Sunaert, S., Todd, J.T., Van Hecke, P., & Marchal, G. (1999). Human cortical regions involved in extracting depth from motion. *Neuron*, *24*, 929–940. doi:10.1016/S0896-6273(00)81040-5

Perry, R.J., & Hodges, J.R. (2003). Dissociation between top-down attentional control and the time course of visual attention as measured by attentional dwell time in patients with mild cognitive impairment. *European Journal of Neuroscience*, *18*, 221–226. doi:10.1046/j.1460-9568.2003.02754.x

Petersen, R.C. (2004). Mild cognitive impairment as a diagnostic entity. *Journal of Internal Medicine*, *256*, 183–194. doi:10.1111/j.1365-2796.2004.01388.x

Petersen, R.C., Doody, R., Kurz, A., Mohs, R.C., Morris, J.C., Rabins, P.V., … Winblad, B. (2001). Current concepts in mild cognitive impairment. *Archives of Neurology*, *58*, 1985–1992. doi:10.1001/archneur.58.12.1985

Petersen, R.C., Smith, G.E., Waring, S.C., Ivnik, R.J., Tangalos, E.G., & Kokmen, E. (1999). Mild cognitive impairment: Clinical characterization and outcome. *Archives of Neurology*, *56*, 303–308. doi:10.1001/archneur.56.3.303

Prvulovic, D., Hubl, D., Sack, A.T., Melillo, L., Maurer, K., Frolich, L., … Dierks, T. (2002). Functional imaging of visuospatial processing in Alzheimer's disease. *Neuroimage*, *17*, 1403–1414. doi:10.1006/nimg.2002.1271

Reuter-Lorenz, P.A., & Park, D.C. (2014). How does it STAC up? Revisiting the scaffolding theory of aging and cognition. *Neuropsychology Review*, *24*, 355–370. doi:10.1007/s11065-014-9270-9

Risacher, S.L., Wudunn, D., Pepin, S.M., MaGee, T.R., McDonald, B.C., Flashman, L.A., … Saykin, A.J. (2013). Visual contrast sensitivity in Alzheimer's disease, mild cognitive impairment, and older adults with cognitive complaints. *Neurobiology of Aging*, *34*, 1133–1144. doi:10.1016/j.neurobiolaging.2012.08.007

Rizzo, M., Anderson, S.W., Dawson, J., & Nawrot, M. (2000). Vision and cognition in Alzheimer's disease. *Neuropsychologia*, *38*, 1157–1169. doi:10.1016/S0028-3932(00)00023-3

Roman, G.C., Tatemichi, T.K., Erkinjuntti, T., Cummings, J.L., Masdeu, J.C., Garcia, J.H., … Hofman, A. (1993). Vascular dementia: Diagnostic criteria for research studies. Report of the NINDS-AIREN International Workshop. *Neurology*, *43*, 250–260. doi:10.1212/WNL.43.2.250

Rose, S.E., McMahon, K.L., Janke, A.L., O'Dowd, B., de Zubicaray, G., Strudwick, M.W., & Chalk, J.B. (2006). Diffusion indices on magnetic resonance imaging and neuropsychological performance in amnestic mild cognitive impairment. *Journal of Neurology, Neurosurgery, & Psychiatry*, *77*, 1122–1128. doi:10.1136/jnnp.2005.074336

Sperling, R. (2011). Potential of functional MRI as a biomarker in early Alzheimer's disease. *Neurobiology of Aging*, *32*(Suppl. 1), S37–S43. doi:10.1016/j.neurobiolaging.2011.09.009

Tales, A., Haworth, J., Nelson, S., Snowden, R.J., & Wilcock, G. (2005). Abnormal visual search in mild cognitive impairment and Alzheimer's disease. *Neurocase*, *11*, 80–84. doi:10.1080/13554790490896974

Teipel, S.J., Bokde, A.L., Born, C., Meindl, T., Reiser, M., Möller, H.J., & Hampel, H. (2007). Morphological substrate of face matching in healthy ageing and mild cognitive impairment: A combined MRI-fMRI study. *Brain*, *130*, 1745–1758. doi:10.1093/brain/awm117

Teipel, S.J., Grothe, M., Lista, S., Toschi, N., Garaci, F.G., & Hampel, H. (2013). Relevance of magnetic resonance imaging for early detection and diagnosis of Alzheimer disease. *Medical Clinics of North America*, *97*, 399–424. doi:10.1016/j.mcna.2012.12.013

Troje, N.F., & Bulthoff, H.H. (1996). Face recognition under varying poses: The role of texture and shape. *Vision Research*, *36*, 1761–1771. doi:10.1016/0042-6989(95)00230-8

Vannini, P., Almkvist, O., Dierks, T., Lehmann, C., & Wahlund, L.O. (2007). Reduced neuronal efficacy in progressive mild cognitive impairment: A prospective fMRI study on visuospatial processing. *Psychiatry Research*, *156*, 43–57. doi:10.1016/j.pscychresns.2007.02.003

Villain, N., Chetelat, G., Desgranges, B., & Eustache, F. (2010). Neuroimaging in Alzheimer's disease: A synthesis and a contribution to the understanding of physiopathological mechanisms. *Biologie Aujourdhui*, *204*, 145–158. doi:10.1051/jbio/2010010

Villain, N., Fouquet, M., Baron, J.C., Mezenge, F., Landeau, B., de La Sayette, V., … Chételat, G. (2010). Sequential relationships between grey matter and white matter atrophy and brain metabolic abnormalities in early Alzheimer's disease. *Brain*, *133*, 3301–3314. doi:10.1093/brain/awq203

Xiao, D.K., Marcar, V.L., Raiguel, S.E., & Orban, G.A. (1997). Selectivity of macaque MT/V5 neurons for surface orientation in depth specified by motion. *European Journal of Neuroscience*, *9*, 956–964. doi:10.1111/j.1460-9568.1997.tb01446.x

Yamasaki, T., Muranaka, H., Kaseda, Y., Mimori, Y., & Tobimatsu, S. (2012). Understanding the pathophysiology of Alzheimer's disease and mild cognitive impairment: A mini review on fMRI and ERP studies. *Neurology Research International*, *2012*, 1–10. doi:10.1155/2012/719056